Table I. Representative ^{13}C and ^{1}H Spin Systems Identified on the Basis of Two-Dimensional ^{13}C–^{13}C and ^{1}H–^{13}C Connectivities

group[a]	carbon atom	chemical shifts[b] (ppm) ^{13}C (±0.1)	attached ^{1}H (±0.02)
ribose	1′	52.2	
	2′	71.2	2.79
	3′	74.6	3.60
	4′	71.0	4.21
	5′	63.8	
isoalloxazine ring	5a	139.4	
	6	129.8	
	7	141.9	
	7a	20.3	
	8	152.8	
	8a	23.0	
alanine-A	o	172.8	
	α	51.2	
	β	21.4	
tyrosine-A	o	171.8	
	α	52.3	
	β	34.9	
	γ	127.7	
	δ	131.4[c]	
	ε	116.0[c]	
	ζ	156.3	
threonine-A	o	170.8	
	α	59.9	
	β	66.3	
	γ	16.4	

[a] Sequence-specific assignments have not been made yet for the amino acid spin systems. [b] ^{13}C chemical shifts are relative to TMS. ^{1}H chemical shifts are relative to TSP. [c] The two tyrosine $^{13}C_\delta$ and $^{13}C_\epsilon$ carbons appear to have degenerate chemical shifts.

At least 154 of the expected ~210 $^{13}C_o$–$^{13}C_\alpha$ correlations were resolved by using the software package MADNMR.[2] This suggests that uniform ^{13}C labeling will support a heteronuclear approach to sequence-specific resonance assignments. The ^{13}C–^{13}C correlations, in combination with multiple-bond ^{13}C–^{1}H correlations or ^{13}C–^{15}N correlations from dual $^{13}C/^{15}N$-labeled proteins, or both, can be used to trace out the peptide backbone connectivities.[1,10,11]

Sensitivity considerations limit the application of the ^{13}C-{^{13}C}DQC experiment to proteins enriched with ^{13}C. Current methods for incorporating stable isotopes into biotechnology derived proteins have begun to alleviate this problem.[12] Carbon-13 enrichment levels of 20–30% represent a good compromise between improved sensitivity and decreased spectral simplicity. Higher enrichment levels might be useful for providing long-range carbon–carbon coupling constants for selectively enriched proteins[1] but would result in increased spectral overlap in a uniformly enriched protein.

Acknowledgment. Supported by USDA Competitive Research Grant 85-CRCR-1-1589. This study made use of the National Magnetic Resonance Facility at Madison which is supported in part by NIH Grant RR02301 from the Biomedical Research Technology Program, Division of Research Resources. Additional equipment in the facility was purchased with funds from the University of Wisconsin, the NSF Biological Biomedical Research Technology Program (DMB-8415048), NIH Shared Instrumentation Program (RR02781), and the U.S. Department of Agriculture. B.J.S. is supported by an NIH Training Grant in Cellular and Molecular Biology (GM07215).

(10) Kainosho, M.; Tsuji, T. *Biochemistry* **1982**, *21*, 6273–6279.
(11) Markley, J. L.; Westler, W. M.; Chan, T.-M.; Kojiro, C. L.; Ulrich, E. L. *Federation Proc.* **1984**, *43*, 2648–2656.
(12) Markley, J. L. In *Protein Engineering*; Oxender, D., Fox, C. F., Eds.; Alan R. Liss: New York, 1987; pp 15–33.
(13) Shaka, A. J.; Keeler, J.; Frenkiel, T.; Freeman, R. *J. Magn. Reson.* **1983**, *52*, 335–338.
(14) Zolnai, Z.; Macura, S.; Markley, J. L. *Comput. Enhanced Spectrosc.* **1986**, *3*, 141–145.

First Direct Observation of Pyridyne: Matrix Infrared Study of the Photolysis Products of 3,4-Pyridine Dicarboxylic Anhydride

H.-H. Nam and G. E. Leroi*

Department of Chemistry, Michigan State University East Lansing, Michigan 48824

Received March 7, 1988

Heteroarynes have been proposed as likely intermediates in many organic reactions, principally those involving cycloaddition or cine-substitution.[1] However, only indirect evidence, based on trapping experiments to verify the presence of heteroaryne intermediacy, has been obtained. The reliability of such inferences is severely limited. Other mechanisms, e.g., addition–elimination, trans-halogenation, or addition ring opening–elimination ring closure(ANRORC), also can account for the formation of observed products.[1] Mass spectrometric analysis following the electron impact or the pyrolytic fragmentation of several heteroarene dicarboxylic anhydrides has been used to conjecture the structure of heteroarynes corresponding to certain m/z peaks.[2-5] Although diazabiphenylene, the dimer of 3,4-pyridyne, has been identified in the time of flight mass spectrometric and kinetic UV spectroscopic analysis of the products formed by flash photolysis of pyridine-3-diazonium-4-carboxylate,[6] no direct observation of any heteroaryne has yet been published.

In this report we present the first infrared spectrum of 3,4-pyridyne (3,4-didehydropyridine), generated via near UV photolysis ($\lambda > 340$ nm) of 3,4-pyridine dicarboxylic anhydride (3,4-PDA) in N_2 or Ar matrices. Similar experiments by Dunkin and McDonald were not successful;[7] apparently the photolytic conditions utilized in that study produced only decomposition products of the desired heteroaryne.

3,4-PDA (obtained from Aldrich and vacuum sublimed before use) was sublimed and codeposited for 2 h with Ar or N_2 (flow rate 2 mmol/min) on the CsI substrate of an Air Products CS202 Displex cryostat. Photolyses were conducted with a 200 W Hg-Xe arc lamp equipped with a water filter and various cutoff filters. Infrared spectra of the precursor and photolyzed products at 13 K were recorded with a BOMEM DA3.01 interferometric spectrometer.

As summarized in Scheme I, mild irradiation ($\lambda > 340$ nm and less than 100 min duration) of 3,4-PDA in N_2 or Ar matrices at 13 K readily fragmented the precursor to form CO, CO_2, and 3,4-pyridyne, which has a strong peak at 2085 cm^{-1} diagnostic of carbon–carbon triple bond formation. Subsequent irradiation with $\lambda > 210$-nm light immediately decomposed 3,4-pyridyne into HCN, diacetylene, acetylene, and cyanoacetylene as a result of alternative two-bond scissions. The infrared spectrum in the 2050–2300 cm^{-1} region prior to and following controlled photolysis (Figure 1) clearly demonstrates the formation of 3,4-pyridyne and its subsequent decomposition. The peak due to 3,4-pyridyne at 2085 cm^{-1} disappears upon shorter wavelength irradiation, and new peaks at 2101 cm^{-1} (HCN), 2181 cm^{-1} (diacetylene) and 2236 cm^{-1} (cyanoacetylene) begin to grow. Ten additional peaks below 2000 cm^{-1} show the same growth and decay pattern as the 2085-cm^{-1} band and are also attributable to 3,4-pyridyne (Table I).

(1) Reinecke, M. G. *Tetrahedron* **1982**, *38*, 427.
(2) Brown, R. F. C.; Crow, W. D.; Solly, R. K. *Chem. Ind. (London)* **1966**, 343.
(3) Cava, M. P.; Mitchell, M. J.; DeJongh, D. C.; van Fossen, R. Y. *Tetrahedron Lett.* **1966**, *26*, 2947.
(4) Reinecke, M. G.; Newsom, J. G.; Chen, L.-J. *J. Am. Chem. Soc.* **1981**, *103*, 2760.
(5) Sio, F.; Chimichi, S.; Nesi, R. *Heterocycles* **1982**, *19*, 1427.
(6) Kramer, J.; Berry, R. S. *J. Am. Chem. Soc.* **1972**, *94*, 8336.
(7) Dunkin, I. R.; McDonald, J. G. *Tetrahedron Lett.* **1982**, *23*, 4839.

0002-7863/88/1510-4096$01.50/0

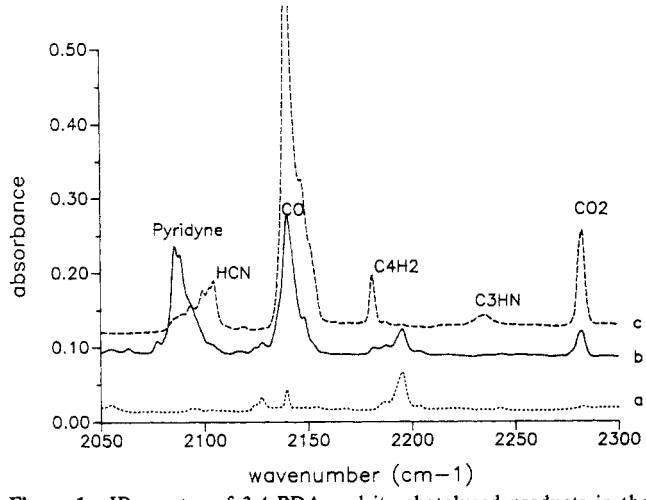

Figure 1. IR spectra of 3,4-PDA and its photolyzed products in the 2050–2300-cm^{-1} region in an N_2 matrix at 13 K: (a) 3,4-PDA; (b) after 100 min photolysis through water and $\lambda > 340$-nm filter (The peak at 2281 cm^{-1} is due to $^{13}CO_2$); (c) following additional 30 min photolysis with $\lambda > 210$ nm.

Table I. Infrared Bands (cm^{-1}) Resulting from Photolysis of 3,4-PDA in an N_2 Matrix at 13 K[d]

$\lambda > 340$ nm[a]	$\lambda > 210$ nm[b]	photolyzed products	*o*-benzyne[c]
	2236	cyanoacetylene	
	2181	diacetylene	
	2101	HCN	
2085		3,4-pyridyne	2082
1558		3,4-pyridyne	1596
			1448
1387		3,4-pyridyne	1395
1355		3,4-pyridyne	1355
	1260	polymer	
1216		3,4-pyridyne	
1055		3,4-pyridyne	1055
			1038
996		3,4-pyridyne	
853		3,4-pyridyne	
848		3,4-pyridyne	848
802		3,4-pyridyne	
	751	acetylene	
744	744	acetylene	
			739
	703	polymer	
	673	cyanoacetylene	
648	648	diacetylene	
635	635	diacetylene	
489		3,4-pyridyne	470

[a] Photolysis of 3,4-PDA. (100 min). [b] Additional 30 min photolysis after *a*. [c] Reference 9. [d] Comparison to *o*-benzyne (last column).

The IR frequencies of 3,4-pyridyne indicate that this molecule is remarkably similar to *o*-benzyne in character. The wavenumbers observed for both *o*-benzyne and 3,4-pyridyne in N_2 matrices are collected in Table I. However, 3,4-pyridyne decomposes much faster. Although crude thermodynamic calculations suggest similar ring strain energy for these two molecules (~60 kcal/mol),[8] 3,4-pyridyne has less resonance energy, which may account for its lower stability.

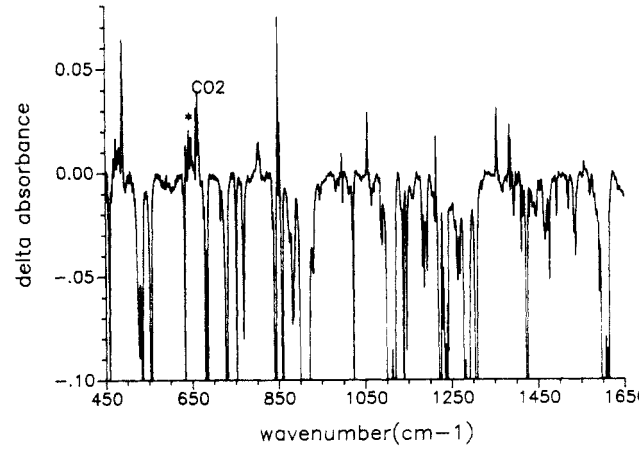

Figure 2. Difference spectrum of 3,4-PDA before and after mild photolysis. * indicates a band due to diacetylene.

Scheme I

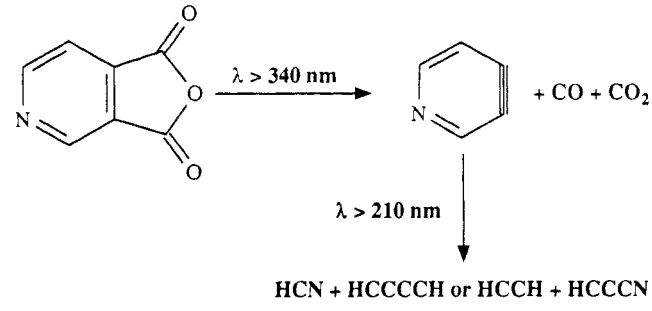

Unlike 3,4-pyridyne, the 2,3-isomer could not be isolated under our experimental conditions. Additional experiments to identify the products of 2,3-PDA photolysis are in progress. The results, plus theoretical calculations of the structures and vibrational frequencies of various heteroarynes, will be reported in a future publication.

Acknowledgment. We thank Professors Harold Hart and James Harrison for their continuing interest in this work. H.-H. Nam was a recipient of a MOBAY Summer Research Fellowship. This research was supported in part by Grant nos. CHE86-10421 and CHE87-22111 from the National Science Foundation.

(8) The theoretically calculated heat of formation of 3,4-pyridyne (Dewar, M. J. S.; Ford, G. P. *J. Chem. Soc., Chem. Commun.* **1977**, 539) was used in this estimation.

(9) Nam, H.-H.; Leroi, G. E. *J. Mol. Struct.* **1987**, *157*, 301.